

# Morphological Effect of Green Synthesis Cerium Oxide Nanoparticles Enhanced Antibacterial Activity

**Gusliani Eka Putri** \*<sup>1</sup>

**Putri Dafriani** <sup>2</sup>

**Ika Yulia Darma** <sup>3</sup>

**Sri Handayani** <sup>4</sup>

**Widyastuti** <sup>5</sup>

**Nor Monica Ahmad** <sup>6</sup>

**Arniati Labanni** <sup>7</sup>

**Syukri Arief** <sup>8</sup>

<sup>1</sup> Department of Biomedical Science, Universitas Syedza Saintika, Padang 25132, Indonesia

<sup>2</sup> Department of Nurse, Universitas Syedza Saintika, Padang 25132, Indonesia

<sup>3</sup> Department of Midwifery, Universitas Syedza Saintika, Padang 25132, Indonesia

<sup>4</sup> Department of Public Health, Universitas Syedza Saintika, Padang 25132, Indonesia

<sup>5</sup> Department of Pharmacy, Universitas Perintis Indonesia, Padang 25586, Indonesia

<sup>6</sup> School of Chemistry and Environment, Faculty of Applied Science, Universiti Teknologi MARA, Kuala Pilah, Negeri Sembilan 72000, Malaysia

<sup>7</sup> Research Center for Environment and Clean Technology, National Research and Innovation Agency of Republic Indonesia (BRIN), KST Samaun Samadikun Bandung 40135, Indonesia

<sup>8</sup> Department of Chemistry, Universitas Andalas, Padang 25163, Indonesia

\*e-mail: guslianiekaputri@gmail.com

---

*Submitted* 9 December 2024

*Revised* 1 August 2025

*Accepted* 15 August 2025

---

**Abstract.** Cerium oxide nanoparticles (CeO<sub>2</sub>NPs) were successfully synthesized using two methods, which are the precipitation and green synthesis. In the green synthesis approach, leaf extracts from *Moringa oleifera* and *Uncaria gambir* Roxb. acted as a natural capping and reducing agents. In contrast, ammonium hydroxide was used in the chemical precipitation method. X-ray diffraction (XRD) analysis confirmed the formation of CeO<sub>2</sub>NPs with a cubic fluorite structure. Scanning electron microscopy (SEM) revealed that the nanoparticles had an agglomerate morphology. In contrast, transmission electron microscopy (TEM) showed that the CeO<sub>2</sub>NPs were predominantly spherical, with average particle sizes of approximately 5–20 nm for the green synthesis method and 10–40 nm for the precipitation method. The antibacterial assays demonstrated significant activity, particularly against *Staphylococcus aureus*, with the inhibition zones measuring up to 11.05 mm. These findings suggest that green-synthesized CeO<sub>2</sub>NPs hold promising potential for applications in the biomedical field due to their biocompatibility and antibacterial properties.

**Keywords:** Antibacterial, Cerium Oxide, Green Synthesis, *Moringa Oleifera*, Precipitation

## INTRODUCTION

Cerium oxide nanoparticles (CeO<sub>2</sub>NPs) have attracted considerable attention in

recent years due to their remarkable oxygen storage capacity, making them highly suitable for applications in many fields (Eka Putri *et al.*, 2019). CeO<sub>2</sub>NPs have oxygen storage

capacity because cerium has two oxidation numbers, namely trivalent  $\text{Ce}^{3+}$  and  $\text{Ce}^{4+}$  tetravalent. Therefore, cerium oxide acts as an oxygen provider in an oxygen-deprived environment. After the oxide surface gives oxygen,  $\text{Ce}^{4+}$  was reduced to  $\text{Ce}^{3+}$  because the extra electrons are left behind (Eka Putri *et al.*, 2021; Putri *et al.*, 2022; Eka Putri *et al.*, 2019). When the oxide surface lacks oxygen,  $\text{Ce}^{3+}$  will tend to receive oxygen again.  $\text{CeO}_2$ NPs can inactivate hydroxyl radicals of superoxide radicals, nitric oxide, and hydrogen peroxide (Sales *et al.*, 2020; Li *et al.*, 2022). A major issue in healthcare is the rapid development of bacterial resistance to antibiotics. To combat this, various strategies aim to create effective antibacterial agents, with  $\text{CeO}_2$ NPs gaining attention for their strong antibacterial properties (Arumugam *et al.*, 2015; G. E. Putri *et al.*, 2019).  $\text{CeO}_2$ NPs exhibit antibacterial activity through the generation of reactive oxygen species (ROS) like superoxide anions and hydroxyl radicals, which damage bacterial cell membranes and cause cell death. The reversible redox cycling between  $\text{Ce}^{3+}$  and  $\text{Ce}^{4+}$  enhances catalytic activity and maintains antibacterial effects, making cerium oxide a promising candidate for antibacterial formulations and biomedical applications (Mohammadi *et al.*, 2019; Kalaycioğlu *et al.*, 2020).

The synthesis of metal oxide nanoparticles has been accomplished using various methods. The use of plant extracts is a common approach, largely due to their availability and the wide range of secondary metabolites they possess, which contribute to various biological activities (Nourmohammadi *et al.*, 2020). These secondary metabolites act as natural reducing and capping agents, and hence are sustainable and less toxic (Iconaru *et al.*, 2021; Hao *et al.*, 2020). In addition, this method can

be scaled up to an industry level (Ramachandran *et al.*, 2019). The use of plant extracts in the synthesis has been described in several publications to synthesis of  $\text{CeO}_2$ NPs, such as Gloriosa superba leaf extract (Arumugam *et al.*, 2015), Acalypha indica leaf extract (Kannan & Sundrarajan, 2014), Aloe vera (Gel *et al.*, 2014), Hibiscus sabdarifa flower extract (Thovhogi *et al.*, 2015), Olei europaea leaf extract (Abid *et al.*, 2022), Sida acuta leaf extract (Senthilkumar *et al.*, 2017), Prosofis juliflora leaf extract (Arunachalam *et al.*, 2017), and Calotropis procera flower extract (Muthuvel *et al.*, 2020; Chavhan *et al.*, 2020).

In this research, we synthesized  $\text{CeO}_2$ NPs using three different methods: the precipitation method, and two green synthesis methods employing *Moringa oleifera* and *Uncaria gambir* Roxb. leaf extract. The precipitation method used a mixed solvent system of propanol and water, with ammonium hydroxide ( $\text{NH}_4\text{OH}$ ) as the precipitating agent. In contrast, the green synthesis methods using *Moringa oleifera* and *Uncaria gambir* Roxb. extracts utilized only water as the solvent, without any chemical precipitating agents. This highlights the potential advantages of green synthesis in terms of cost-effectiveness and environmental sustainability. Consequently, the study aimed to evaluate the benefits of green synthesis in comparison to the conventional chemical approach.

## MATERIALS AND METHODS

### Chemicals and Reagents

Precursor used cerium (III) nitrate hexahydrate ( $\text{Ce}(\text{NO}_3)_3 \cdot 6\text{H}_2\text{O}$ ) 99% trace metal basis from Sigma Aldrich, ammonium hydroxide ( $\text{NH}_4\text{OH}$ ) from Sigma Aldrich, used

to control pH of the solution in the precipitation method. Isopropanol from Sigma Aldrich and deionized water as solvents in the precipitation method. *Uncaria gambir* Roxb. and *Moringa oleifera* leaf from the Biological Education and Research Forest of Andalas University, Sumatra Barat, Indonesia.

### Synthesis of Cerium Oxide Nanoparticles with the Precipitation Method

Synthesis of CeO<sub>2</sub>NPs under typical synthetic conditions, 1.07 g Ce (NO<sub>3</sub>)<sub>3</sub>.6H<sub>2</sub>O was added to a solvent combination of isopropanol and deionized water (3:1), homogenized using magnetic stirring. The pH of the solution was adjusted (around pH ≈ 9–10) using NH<sub>4</sub>OH. The stirring of the solution continues for 24 h; then, it has been transferred into a polypropylene (PP) bottle. The PP bottle was then placed in the oven at 100 °C for 72 h, filtered, and calcined at 600 °C for 2 hours.

### Synthesis of Cerium Oxide Nanoparticles with *Uncaria gambir* Roxb. Leaf Extract

Cerium oxide nanoparticles were synthesized via the hydrothermal method using NaOH as an oxidizing agent and *Uncaria gambir* Roxb. leaf extract as a capping agent. The synthesis of cerium oxide nanoparticles was started by dissolving 1.74 grams of Ce(NO<sub>3</sub>)<sub>3</sub>.6H<sub>2</sub>O in 75 mL of 6.4M NaOH and 10 mL *Uncaria gambir* Roxb. leaf extract. After that, the mixture was stirred for 30 minutes and homogenized by ultrasonication for 10 minutes. Then the hydrothermal process on the mixture was carried out at 150 °C for 24 hours. The precipitate was then washed with ethanol and distilled water 3 times. Then the precipitate was dried at 105 °C for 12 hours.

### Synthesis of Cerium Oxide Nanoparticle with *Moringa oleifera* Leaf Extract

A total of 3.72 g of cerium nitrate hexahydrate was added to 50 mL of *M. oleifera* leaf extract. The solution was stirred using a magnetic stirrer at 80 °C for 2 hours, until the solution changed color from dark brown to light brown. The resulting solid was calcined at 600 °C for 2 hours, to obtain CeO<sub>2</sub>NPs.

### Antibacterial Activity

The antibacterial activity of CeO<sub>2</sub>NPs was evaluated against *Staphylococcus aureus* (Gram-positive) and *Escherichia coli* (Gram-negative) using the disc diffusion method. Mueller Hinton Agar (MHA) was poured into Petri dishes (20 mL each) and allowed to solidify. Then, 1 mL of the overnight bacterial culture was spread on the agar surface. Discs loaded with CeO<sub>2</sub>NPs at concentrations of 25%, 50%, 75%, and 100% were placed on the plates, along with amoxicillin as a positive control, DMSO as a negative control. After 24 hours of incubation at 37 °C, inhibition zones were measured. Clear zones around the discs indicated antibacterial activity.

### Characterization of CeO<sub>2</sub>NPs Nanoparticles

The morphology of CeO<sub>2</sub>NPs was analyzed using scanning electron microscope (SEM) (JEOL JSM IT300 microscope) operating at 20 kV and transmission electron microscope (TEM) JEOL JEM-2100 / FEI Tecnai G2 Spirit / Hitachi HT7700. Functional groups contained in the sample were analyzed using Fourier transform infrared spectroscopy (FTIR) (JEOL JSM 6950) in the 400–4000 cm<sup>-1</sup> wavenumber range. The crystal structure of the resulting CeO<sub>2</sub>NPs was determined using X-ray diffraction (XRD) (XPert Pro Panalytical PW 30/60) with a

graphite monochromator of  $\text{CuK}\alpha$  radiation. To calculate the crystallite size of  $\text{CeO}_2$ NPs, Scherrer's equation was used.

## RESULTS AND DISCUSSION

### XRD Analysis

The XRD pattern of the precipitation method, *Uncaria gambir* Roxb. leaf extract, and *Moringa oleifera* leaf extract mediated synthesized  $\text{CeO}_2$ NPs are shown in Figure 1. It shows the appearance of specific peaks in  $2\theta$  of  $28.55^\circ$ ,  $33.08^\circ$ ,  $47.47^\circ$ ,  $56.33^\circ$ ,  $59.08^\circ$ ,  $69.40^\circ$ ,  $76.69^\circ$ , and  $79.07^\circ$  without any impurities. This pattern refers to cubic  $\text{CeO}_2$ NPs with hkl of (111), (200), (220), (311), (222), (400), (331), and (420), respectively, based on ICSD standard No 34-0394.

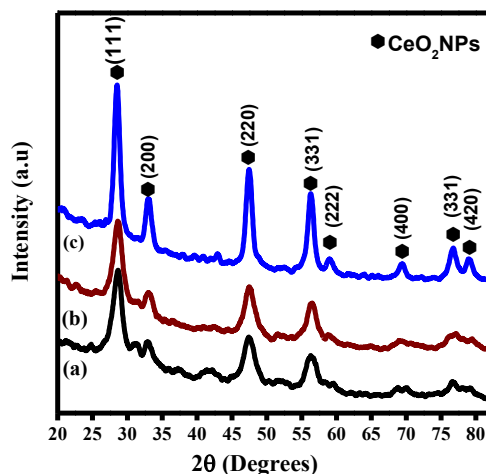


**Fig. 1:** XRD analysis of  $\text{CeO}_2$ NPs used (a) Precipitation Method, (b) *Uncaria gambir* Roxb. leaf extract, (c) *Moringa oleifera* leaf extract

The crystalline phase and structure of the synthesized  $\text{CeO}_2$ NPs were investigated using X-ray diffraction techniques to properly study the position of the atoms in the cubic structure. Figure 1 shows the XRD patterns of  $\text{CeO}_2$ NPs nanoparticles produced from Ammonium hydroxide, *Uncaria gambir* Roxb., and *Moringa* aqueous extract as a capping

agent. No significant characteristic peaks appear from Ce or other impurities detected on the diffractogram, indicating the high purity of the synthesized  $\text{CeO}_2$ NPs nanoparticles.

The average diameter of crystalline (D) was measured using Scherrer's formula (Eq. (1)).

$$D = \frac{\kappa\lambda}{\beta \cos\theta} \quad (1)$$

The crystallite size (D) was calculated using the Scherrer equation of Eq. (1), where  $K$  is a dimensionless shape factor that depends on the crystallite geometry (typically 0.9),  $\lambda$  is the X-ray wavelength,  $\beta$  is the full width at half maximum (FWHM) of the selected diffraction peak in radians, and  $\theta$  is the Bragg angle corresponding to that peak.

These findings align with Khaoula Hkiri (Hkiri *et al.*, 2024), where cerium oxide nanoparticles synthesized using *Portulaca oleracea* extract exhibited a cubic crystal system and an average crystallite size of 25–35 nm. The smaller crystallite size in their study may result from specific antioxidants and capping agents in the extract, which limit particle growth during synthesis. This consistency across green synthesis methods suggests that plant-mediated synthesis is an effective approach for producing crystalline  $\text{CeO}_2$  nanoparticles with desirable structural characteristics. The results indicate that natural phytochemicals significantly influence nanoparticle formation while ensuring phase purity and crystallinity.

### Morphological Analysis

Sample characterization using SEM shows the morphology and topography of the sample. Figure 2 shows SEM images  $\text{CeO}_2$ NPs synthesized via three methods: (A) precipitation, (B) *Uncaria gambir* Roxb. leaf

extract, and (C) *Moringa oleifera* leaf extract. In Figure 2(A), the nanoparticles from the precipitation method are large, irregular agglomerates with rough surfaces and average sizes over 50 nm, indicating uncontrolled growth. Figure 2(B) displays nanoparticles produced using *Uncaria gambir*, which are smaller and plate-like due to phytochemicals that reduce agglomeration. Figure 2(C) shows nanoparticles from *Moringa oleifera* that are more uniform and faceted, benefiting from better stabilization by flavonoids and polyphenols during growth, resulting in finer, more crystalline structures.

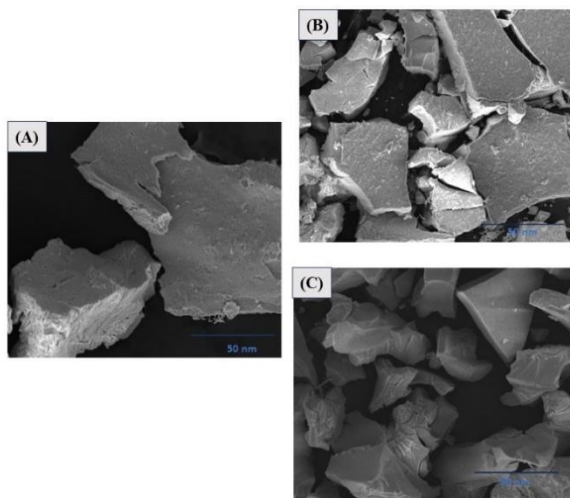


**Fig. 2:** SEM Morphological analysis of CeO<sub>2</sub>NPs used (A) Precipitation method (B) *Uncaria gambir* Roxb. leaf extract (C) *Moringa oleifera* leaf extract

The crystallographic and morphological characteristics of cerium oxide nanoparticles synthesized using three different methods are summarized in Table 1. All samples exhibit a cubic crystal system, which is typical for CeO<sub>2</sub> nanoparticles and confirms the successful formation of the fluorite structure.

In terms of crystallite size (D) in Table 1, the nanoparticles synthesized with other methods range from 10 to 50 nm. The CeO<sub>2</sub>

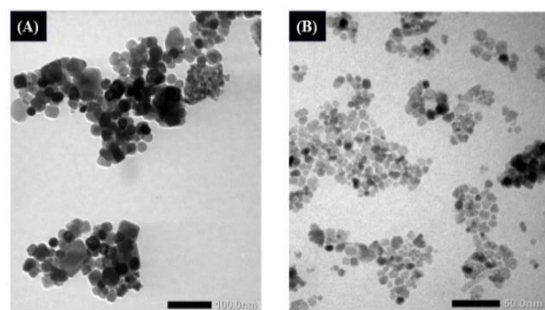
nanoparticles synthesized using *Uncaria gambir* Roxb. leaf extract exhibited slightly larger crystallite sizes (40–50 nm) compared to the *Moringa oleifera*-based sample (30–40 nm). The larger D value in the gambir-based synthesis may result from a slower nucleation rate or weaker capping activity of the phytochemicals compared to Moringa. However, both green synthesis methods yielded smaller particle sizes (30–70 nm) than the conventional precipitation approach, indicating better dispersion and stabilization of particles by the plant-derived bioactive compounds.

**Table 1.** Comparison of the XRD and SEM data of the Synthesis of Cerium Oxide nanoparticles using Precipitation Method, *Moringa oleifera* leaf extract, and *Uncaria gambir* Roxb. leaf extract

	<i>Moringa oleifera</i> leaf extract	<i>Uncaria gambir</i> Roxb. leaf extract	Precipitation Method
Crystal system	Cubic	Cubic	Cubic
Diameter of crystalline (D) (nm)	30-40	40-50	30-40
Diameter of particles (nm) in SEM	30-50	40-70	40-80

Notably, *Moringa oleifera* extract resulted in the smallest and most uniform particle sizes (30–50 nm), suggesting a more effective capping and stabilization process, likely due to its rich content of flavonoids, polyphenols, and antioxidants. This comparative analysis supports the potential of plant-mediated green synthesis for controlling particle size and minimizing agglomeration in CeO<sub>2</sub> nanoparticle production, with *Moringa oleifera* showing the most promising performance among the tested methods. Based on this condition, in Figure 3 in this

manuscript, only the TEM results of the precipitation method and the green synthesis method with *Moringa oleifera* leaf extract are compared.



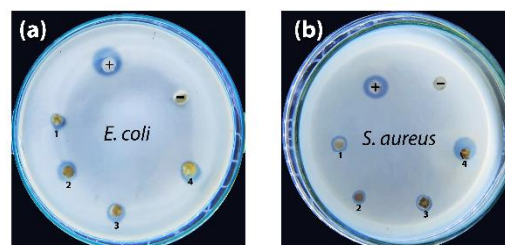
**Fig. 3:** TEM Image of morphological analysis of CeO<sub>2</sub>NPs used (A) precipitation method (B) *Moringa oleifera* leaf extract

Figure 3 shows Transmission Electron Microscopy (TEM) images of CeO<sub>2</sub> nanoparticles (CeO<sub>2</sub>NPs) synthesized via the precipitation method and green synthesis using *Moringa oleifera* extract. In Figure 3(A), the nanoparticles from the precipitation method display irregular, agglomerated particles with a size range of 10-40 nm, indicating poor dispersion. In contrast, Figure 3(B) reveals CeO<sub>2</sub>NPs synthesized with *Moringa oleifera* extract, which are more uniformly distributed, smaller, and spherical, averaging 5-20 nm. This suggests that the green synthesis method yields better control over particle morphology and distribution due to the stabilizing effects of the phytochemicals in the extract. This research aligned the synthesis of CeO<sub>2</sub>NPs using *Portulaca oleracea* extract with sizes ranging from 4 nm to 14 nm (Hkiri *et al.*, 2024).

### Antibacterial Activity

The particle size of nanomaterials affects antibacterial activity. The particle size of the cerium oxide nanoparticles is smaller when using *Moringa oleifera* leaf extract as a capping agent. Based on this condition,

cerium oxide was synthesized using *Moringa oleifera* leaf extract as CeO<sub>2</sub>NPs for antibacterial activity. These nanoparticles are used to test antibacterial properties against Gram-positive bacteria (*S. aureus*) and Gram-negative bacteria (*E. coli*).



**Fig. 4:** Antibacterial activity of CeO<sub>2</sub>NPs with varying concentrations, 25% (1), 50% (2), 75% (3), and 100% (4) against (a) *E. coli* and (b) *S. aureus*.

The antibacterial activity of synthesized cerium oxide nanoparticles (CeO<sub>2</sub>NPs) was assessed against *Escherichia coli* and *Staphylococcus aureus* using the disc diffusion method. Results, as indicated in Table 2, showed a concentration-dependent antibacterial effect, with inhibition zones for *E. coli* ranging from  $4.23 \pm 0.6$  mm at a 25% concentration to  $8.46 \pm 0.6$  mm at a 100% concentration. For *S. aureus*, zones increased from  $4.50 \pm 0.2$  mm to  $11.05 \pm 0.3$  mm as concentration rose, showing that higher concentrations are more effective.

CeO<sub>2</sub>NPs exhibited greater antibacterial activity against *S. aureus* compared to *E. coli*, particularly at 100%, likely due to differences in cell wall structures. The positive control (standard antibiotic) produced inhibition zones of  $12.45 \pm 0.3$  mm for *E. coli* and  $13.56 \pm 0.5$  mm for *S. aureus*, respectively.

The antibacterial activity of CeO<sub>2</sub>NPs is partly due to having two oxidation states, Ce<sup>3+</sup> and Ce<sup>4+</sup>, so that it can produce hydroxyl radicals, which can damage the bacterial cell wall, disrupt cell metabolism, and inhibit

bacterial cell synthesis. Cerium oxide nanoparticles have antibacterial activity due to their large surface area, which allows for excellent contact with microorganisms. Cerium oxide nanoparticles approach the bacterial cell membrane and penetrate the bacteria. The redox state of the Ce<sup>3+</sup> and Ce<sup>4+</sup> nanoparticles diffuses and attacks the bacterial respiratory chain, ultimately leading to cell death. The antibacterial properties of Ce<sup>3+</sup> and Ce<sup>4+</sup> nanoparticles will be very helpful in overcoming various health problems (Eka Putri *et al.*, 2018; Gusliani Eka Putri *et al.*, 2019; You *et al.*, 2023).

**Table 2.** The zone of Inhibition of CeO<sub>2</sub>NPs against *Escherichia coli* and *Staphylococcus aureus* bacteria

Samples	Zone of Inhibition (mm)	
	<i>E. coli</i>	<i>S. aureus</i>
Negative Control	-	-
Positive Control	12.45 ± 0.3	13.56 ± 0.5
CeO <sub>2</sub> NPs 25% (1)	4.23 ± 0.6	4.50 ± 0.2
CeO <sub>2</sub> NPs 50% (2)	6.50 ± 0.5	5.86 ± 0.6
CeO <sub>2</sub> NPs 75% (3)	7.28 ± 0.4	7.40 ± 0.5
CeO <sub>2</sub> NPs 100% (4)	8.46 ± 0.6	11.05 ± 0.3

## CONCLUSIONS

Cerium oxide nanoparticles (CeO<sub>2</sub>NPs) were successfully synthesized using aqueous extracts from the leaves of *Moringa oleifera* and *Uncaria gambir* Roxb. as eco-friendly capping and reducing agents. Structural and morphological analyses confirmed the formation of spherical and moderately agglomerated CeO<sub>2</sub>NPs. The biosynthesized nanoparticles demonstrated significant antibacterial activity, with inhibition zones measuring up to 11.05 mm against *Staphylococcus aureus* and 8.46 mm against *Escherichia coli*, showcasing their effective antimicrobial properties. The use of dual

plant extracts in this green synthesis approach highlights the novelty of this research, the potential of CeO<sub>2</sub>NPs as promising candidates for future biomedical applications, particularly in antimicrobial formulations.

## ACKNOWLEDGEMENTS

This research received funding for Fundamental Research from the Directorate of Research and Community Service of the Republic of Indonesia with grant number [131/C3/DT.05.00/PL/2025].

## REFERENCES

Abid, N., Khan, A.M., Shujait, S., Chaudhary, K., Ikram, M., Imran, M., Haider, J., Khan, M., Khan, Q., and Maqbool, M., 2022. "Synthesis of nanomaterials using various top-down and bottom-up approaches, influencing factors, advantages, and disadvantages: A review." *Adv. Colloid Interface Sci.* 300, 102597. <https://doi.org/10.1016/j.cis.2021.102597>

Arumugam, A., Karthikeyan, C., Haja Hameed, A.S., Gopinath, K., Gowri, S., and Karthika, V., 2015. "Synthesis of cerium oxide nanoparticles using Gloriosa superba L. leaf extract and their structural, optical and antibacterial properties." *Mater. Sci. Eng. C* 49, 408–415. <https://doi.org/10.1016/j.msec.2015.01.042>

Arunachalam, T., Karpagasundaram, U., and Rajarathinam, N., 2017. "Ultrasound assisted green synthesis of cerium oxide nanoparticles using *Prosopis juliflora* leaf extract and their structural, optical and antibacterial properties." *Mater. Sci.-*

Poland 35, 791–798. 2019, 128–140. <https://doi.org/10.1515/msp-2017-0104>

Chavhan, M.P., Lu, C.H., and Som, S., 2020. "Urea and surfactant assisted hydrothermal growth of ceria nanoparticles." *Colloids Surf. A: Physicochem. Eng. Asp.* 601, 124944. <https://doi.org/10.1016/j.colsurfa.2020.124944>

Eka Putri, G., Arief, S., Jamarun, N., Gusti, F.R., and Novita Sary, A., 2018. "Characterization of enhanced antibacterial effects of silver loaded cerium oxide catalyst." *Orient. J Chem.* 34, 2895–2901. <https://doi.org/10.13005/ojc/340629>

Eka Putri, G., Rahayu Gusti, F., Novita Sary, A., and Zainul, R., 2019. "Synthesis of silver nanoparticles used chemical reduction method by glucose as reducing agent." *J. Phys. Conf. Ser.* 1317, 012027. <https://doi.org/10.1088/1742-6596/1317/1/012027>

Eka Putri, G., Rilda, Y., Syukri, S., Labanni, A., and Arief, S., 2021. "Highly antimicrobial activity of cerium oxide nanoparticles synthesized using *Moringa oleifera* leaf extract by a rapid green precipitation method." *J. Mater. Res. Technol.* 15, 2355–2364. <https://doi.org/10.1016/j.jmrt.2021.09.075>

Gel, B.M., Priya, G.S., Kanneganti, A., Kumar, K.A., Rao, K.V., and Bykkam, S., 2014. "Bio synthesis of cerium oxide nanoparticles using aloe barbadensis miller gel." *Int. J. Sci. Res. Pub.* 4, 1–4.

Gusliani Eka Putri, Syukri Arief, Nokesar Jamarun, Feni Rahayu Gusti, and Adel Fisli, 2019. "High performance of photocatalytic activity of cerium doped silica mesoporous operating under visible light irradiation." *Knowledge E* 2019, 128–140. <https://doi.org/10.18502/keg.v1i2.4438>

Hao, D., Zhang, G., Gong, Y., and Ma, Z., 2020. "Development and biological evaluation of cerium oxide loaded polycaprolactone dressing on cutaneous wound healing in nursing care." *Mater. Lett.* 265, 127401. <https://doi.org/10.1016/J.MATLET.2020.127401>

Hkiri, K., Elsayed Ahmed Mohamed, H., Ghotekar, S., and Maaza, M., 2024. "Green synthesis of cerium oxide nanoparticles using *Portulaca oleracea* Extract: Photocatalytic activities." *Inorg. Chem. Commun.* 162, 112243. <https://doi.org/10.1016/J.INOCHE.2024.112243>

Iconaru, S.L., Predoi, M.V., Chapon, P., Gaiaschi, S., Rokosz, K., Raaen, S., Motelica-Heino, M., and Predoi, D., 2021. "Investigation of spin coating cerium-doped hydroxyapatite thin films with antifungal properties." *Coatings* 11 (4), 464. <https://doi.org/10.3390/coatings11040464>

Kalaycıoğlu, Z., Kahya, N., Adımcılar, V., Kaygusuz, H., Torlak, E., Akın-Evingür, G., and Erim, F.B., 2020. "Antibacterial nano cerium oxide/chitosan/cellulose acetate composite films as potential wound dressing." *Eur. Polym. J.* 133, 109777. <https://doi.org/10.1016/j.eurpolymj.2020.109777>

Kannan, S.K., and Sundrarajan, M., 2014. "A green approach for the synthesis of a cerium oxide nanoparticle: Characterization and antibacterial activity." *Int. J. Nanosci.* 13, 1–7. <https://doi.org/10.1142/S0219581X14500185>

Li, H., Wei, M., Lv, X., Hu, Y., Shao, J., Song, X., Yang, D., Wang, W., Li, B., and Dong, X.,

2022. "Cerium-based nanoparticles for cancer photodynamic therapy." *J. Innov. Opt. Health Sci.* 15, 1–13. <https://doi.org/10.1142/S1793545822230099>

Mohammadi, I., Izadi, M., Shahrabi, T., Fathi, D., and Fateh, A., 2019. "Enhanced epoxy coating based on cerium loaded Na-montmorillonite as active anti-corrosive nano reservoirs for corrosion protection of mild steel: Synthesis, characterization, and electrochemical behavior." *Prog. Org. Coat.* 131, 119–130. <https://doi.org/10.1016/j.porgcoat.2019.02.016>

Muthuvel, A., Jothibas, M., Mohana, V., and Manoharan, C., 2020. "Green synthesis of cerium oxide nanoparticles using Calotropis procera flower extract and their photocatalytic degradation and antibacterial activity." *Inorg. Chem. Commun.* 119, 108086. <https://doi.org/10.1016/j.inoche.2020.108086>

Nourmohammadi, E., Khoshdel-sarkarizi, H., Nedaeinia, R., Darroudi, M., and Kazemi Oskuee, R., 2020. "Cerium oxide nanoparticles: A promising tool for the treatment of fibrosarcoma in-vivo." *Mater. Sci. Eng. C* 109, 110533. <https://doi.org/10.1016/j.msec.2019.110533>

Putri, G. E., Arief, S., Jamarun, N., Gusti, F.R., and Zainul, R., 2019. "Microstructural analysis and optical properties of nanocrystalline cerium oxides synthesized by precipitation method." *Rasayan J. Chem.* 12, 85–90. <https://doi.org/10.31788/RJC.2019.1215029>

Putri, Gusliani Eka, Gusti, F.R., Sary, A.N., Arief, S., Jamarun, N., and Syamsul Amar, B., 2019. "Synthesis and antimicrobial activity of cerium oxide/AG dopes silica mesoporous modification as nanofillers for food packaging applications." *Malaysi. Appl. Biol.* 48, 25–32.

Putri, G.E., Rilda, Y., Syukri, S., Labanni, A., and Arief, S., 2022. "Enhancing morphological and optical properties of montmorillonite/chitosan-modified cerium oxide nanoparticles for antimicrobial applications." *Surf. Interfaces* 32, 102166. <https://doi.org/10.1016/j.surfin.2022.102166>

Ramachandran, M., Subadevi, R., and Sivakumar, M., 2019. "Role of pH on synthesis and characterization of cerium oxide (CeO<sub>2</sub>) nano particles by modified co-precipitation method." *Vacuum* 161, 220–224. <https://doi.org/10.1016/j.vacuum.2018.12.002>

Sales, D.A., Marques, T.M.F., Ghosh, A., Gusmão, S.B.S., Vasconcelos, T.L., Luz-Lima, C., Ferreira, O.P., Hollanda, L.M., Lima, I.S., Silva-Filho, E.C., Dittz, D., Lobo, A.O., and Viana, B.C., 2020. "Synthesis of silver-cerium titanate nanotubes and their surface properties and antibacterial applications." *Mater. Sci. Eng. C* 115, 111051. <https://doi.org/10.1016/j.msec.2020.111051>

Senthilkumar, R.P., Bhuvaneshwari, V., Ranjithkumar, R., Sathiyavimal, S., Malayaman, V., and Chandarshekar, B., 2017. "Synthesis, characterization and antibacterial activity of hybrid chitosan-cerium oxide nanoparticles: As a bionanomaterials." *Int. J. Biol. Macromol.* 104, 1746–1752. <https://doi.org/10.1016/j.ijbiomac.2017.03.139>

Thovhogi, N., Diallo, A., Gurib-Fakim, A., and

Maaza, M., 2015. "Nanoparticles green synthesis by Hibiscus Sabdariffa flower extract: Main physical properties." *J. Alloys and Compd.* 647, 392–396.  
<https://doi.org/10.1016/j.jallcom.2015.06.076>

Putri, G. A., Rilda, Y., Syukri, S., Arief, S., 2023. "Hybrid cerium oxide doped montmorillonite / chitosan nanocomposites with hydrothermal method." *AIP Conf. Proc.* 2619, 040004.  
<https://doi.org/10.1063/5.0122641>